

## Experimental investigation of intrinsic thermoacoustic instabilities in a combustion chamber terminated by a variable aperture

Manmohan Vishwakarma<sup>1</sup>; Sathesh Mariappan<sup>2</sup>; Maria Heckl<sup>3</sup>

<sup>1</sup>PhD student, Indian Institute of technology Kanpur, Kanpur, India

<sup>2</sup>Associate professor, Indian Institute of Technology Kanpur, Kanpur, India

<sup>3</sup>Professor, Keele University, UK

### ABSTRACT

Combustion instabilities arise due to flame-acoustic coupling. In experimental studies using laboratory test rigs, the exhaust is typically an open tube end. Acoustic waves are reflected at such an end with only minor losses and form a standing wave that interacts with the flame. If the exhaust is fitted with an aperture, the acoustic losses are enhanced, and intrinsic thermoacoustic modes are likely to manifest themselves. This paper presents an experimental study where the area ratio,  $AR$  (area of aperture to cross-sectional area of combustion chamber) is used as a bifurcation parameter, and the frequency spectra of the acoustic field are recorded.  $AR$  is varied in the range from 1 (fully open end) to 0.02 (nearly closed end). Another parameter of interest is the mean flow velocity. The test rig is a swirl-stabilized premixed combustor with a settling chamber, burner and combustion chamber. The fuel is Liquefied petroleum gas. From the properties of the observed spectra, and from the measurements of the reflection coefficient at the exhaust, a network model is developed. This makes it possible to predict which type of mode will occur, and to calculate its frequency and growth rate.

Keywords: Thermoacoustic, Area ratio, Acoustic losses

### 1. INTRODUCTION

Combustion instability is a significant concern for the development and design of gas turbine engines. In the past, many investigations have been performed for a better understanding of combustion instability. Experimental investigations give real-time data for the study, and modeling allows to understand the physics involved in it [1]. Self-excited instability arises due to an interaction between unsteady heat release rate from the flame and flow perturbations, in particular, acoustic waves inside the combustor. The flame inside the combustor acts as an acoustic source and feeds energy into the system. The generated acoustic waves reflect from the exit of the combustor, perturbing the flame, thus creating a feedback loop inside the combustor, which evolves in acoustically driven instability [2]. In a recent study by Hoeijmakers et al., [3] the exit acoustic boundary condition was close to anechoic, the feedback response for acoustic driven instability was cut-off. Even then, instability appeared due to velocity sensitive flames and was named as intrinsic thermoacoustic (ITA) instability. Therefore, the exit acoustic boundary condition plays a crucial role in identifying the interaction between acoustic waves and flame inside the combustor.

In gas turbine engines, the combustor is followed by turbine blades at the exit, which in real case changes the exit area of the combustor. Many recent studies have already revealed the effect of boundary conditions on the instability [4]. Flame responds to the acoustic waves generated inside the duct. An experimental study performed by Murugesan et al., [5] on two different area ratios,  $AR$  (cross-section area of exit to the cross-sectional area of the combustion chamber) showed the effect of acoustic boundary condition on flame-acoustic interaction. ITA mode of instability was discussed in the same study. This instability was further identified due to the interaction of flame and acoustic waves traveling upstream. The corresponding boundary condition at the exit was close to anechoic. The study was limited to two  $AR$ . A systematic investigation is required in which the exit is fitted with

<sup>1</sup> mohanv@iitk.ac.in

<sup>2</sup> sathesh@iitk.ac.in

<sup>3</sup> m.a.heckl@keele.ac.uk

a variable area aperture. In the present study, we focus on the investigation of changing the acoustic boundary condition by fixing the combustor exit with a variable area aperture (valve), in which the exit area can be adjusted. A change in the area changes the reflection coefficient at the exit.

In the past, the reflection coefficient at the exit of the duct with uniform geometry had been studied thoroughly. In a theoretical investigation, Levine et al., [6] identified the effect of frequency on the reflection coefficient of an un-flanged open end. Kariko et al., [7] analyzed Laval nozzles with area variation with non-zero mean flow. They used the concept of acoustic conductivity of the nozzle, which gives the relation between phase shifts of pressure to velocity fluctuations. In turn, acoustic conductivity is directly related to the reflection coefficient of the nozzle. In a theoretical and experimental study by Johnston et al., [8] in 1977, they devised a new impedance tube method for determination of reflection coefficient at the boundary, which is fixed with orifice obstruction, nozzle. The reflection coefficient was found to be independent of the flow inside the duct. In a theoretical study, Cargill [9] used a theoretical model to study the effect of sound radiation from a duct. The energy reflected from the exit boundary is compared with that of Levine [6] for open end. In the same study, the effect of Mach number on the reflection coefficient was investigated. In an experimental study, Poinsot et al., [10] explained that the coupling between acoustic modes and combustion instabilities is affected by the reflection coefficient at the exit. Davies et al., [11] in their numerical study, investigated the effect of different discontinuities in the cross-section geometries on reflection coefficient. In a computational study conducted by Norris et al., [12], they determined the impact of flanged and un-flanged ends on reflection coefficient.

In a gas turbine engine, turbine blades are fixed at the exit of the combustor, which leads to an effective reduction in the exit area (reduction in  $AR$ ). This change in  $AR$  at the exit changes the reflection coefficient at the exit. The change in reflection coefficient at the combustor exit affects the acoustic energy inside the combustor, which in turn affects the physical phenomenon for combustion instability. The mechanism of combustion instability strongly depends on the boundary condition at the exit [13].

In the present study, two microphone technique (14-16) is used to determine the reflection coefficient at the exit of a combustor. Four microphones are fixed at different axial locations of the combustor. The exit area is changed by setting a variable aperture (using a gate valve) at the exit. Experimental determination of reflection coefficient as a function of  $AR$ , frequency, and Mach number is the main focus of the present study.

**2. EXPERIMENTAL SETUP**

Experiments are performed on a test rig, as shown in figure 1. It consists of a settling chamber, mixing tube, swirled, primary combustor and extension ducts. Three driver units are fixed at the settling chamber kept at 60 degrees apart from each other, as shown in figure 1. Driver units are excited using a RIGOL DG1022 signal generator, in the frequency range 40-800Hz. The output of the signal generator is connected to an amplifier (Ahuja SSA-500EM) of 500W.

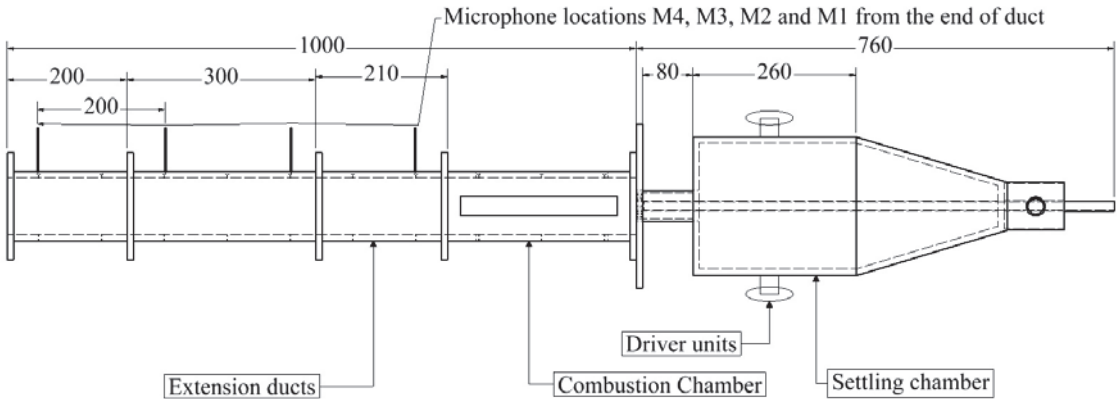


Figure 1: Schematic of the experimental set up. Microphones are placed in M4, M3, M2 and M1 sequence from the exit of duct (from left side of figure)

The amplifier controls the excitation amplitude. Four microphones M1, M2, M3, and M4, mounted in a cooling jacket are installed at different axial locations (indicated in figure 1) from the exit. The axial distance between the two microphones is 200mm, which is found to be an optimum value for the high-frequency range, as suggested in [16]. A semi-infinite tube (6 m long) is connected to the microphones mounting to prevent the occurrence of acoustic resonance within the mount. A description of data acquisition (DAQ) system and data processing is explained elsewhere [16].

## 2.1 Area ratio (AR) calculations:

Figure 2(a) shows the variable aperture gate valve fixed at the end of the duct (shown in figure 1) to reduce the area at exit. The area ratio ( $AR = \text{exit area}/\text{cross section of combustor}$ ) is kept varying with each rotation. Figure 2(b), shows the variation of  $AR$  with rotation.

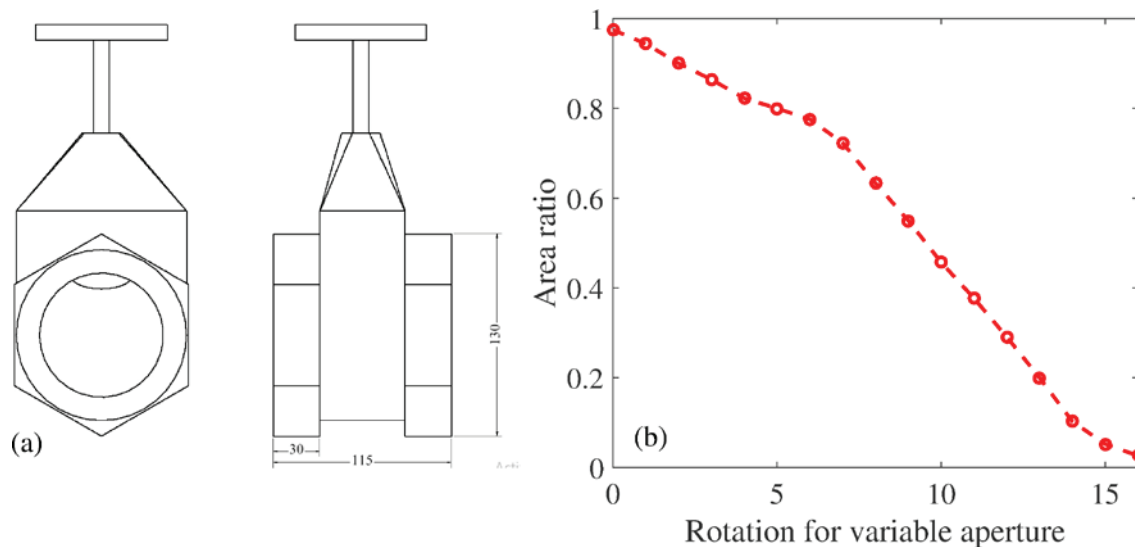


Figure 2(a): Shows the valve used for varying the exit area, Figure 2(b): Area ratio ( $AR$ ) versus rotation of the valve.

The frequency of interest in the present investigation is in the range 40-800Hz, which is much below the cutoff frequency ( $f_{cut}$ ). In the present case,  $f_{cut}$  for the propagation of a non-planar mode (radial mode) is 1.8kHz ( $f_{cut} = 1.84 * a / (2 * \pi * d_{cut} / 2)$ ); hence, only longitudinal modes propagate in the duct. The settling chamber works as Helmholtz resonator, with the mixing tube (figure 1) acts as a neck. Previous calculations show that the associated frequency is 72.73Hz.

## 3. RESULTS AND DISCUSSION

Experiments are performed on the set up shown in figure 1 for the open end (absence of gate valve). The results for the open end are explained in section 3.1. Variable aperture (gate valve), shown in figure 2(a), is then fixed at the end of open for changing the exit area. The results for various  $AR$  are illustrated in section 3.2. The variable aperture experiment is performed for two different air flow rates: 200 and 600slpm. Section 3.3 compares the reflection coefficient for the two air flow rates. Section 3.4 shows the reflection coefficient variation with  $AR$ . The presence of laboratory walls [16] on reflection coefficient is found to alter the value by less than 1%, and therefore, their effects are neglected.

### 3.1 Variation of reflection coefficient for open end condition of the duct

In figure 3, experimentally determined values of the reflection coefficient are compared with the existing theoretical results [6]. In a practical case, the waves inside the duct are the combination of traveling and standing waves[11]. From the past studies [6] it has been observed that the reflection coefficient decreases with frequency at the exit for a uniform geometry. Figure 3(a) shows the variation of modulus of reflection coefficient ( $|R|$ ) with frequency.  $|R|$  decreases with increase in frequency up to 220Hz. At 380, 460 and 680Hz,  $|R|$  is much lesser compared to other values which indicate higher loss of acoustic energy.

The phase value for a reflected wave at the exit is normalized by  $\pi$  radian. In figure 3(b), the

phase( $\theta/\pi$ ) decreases with frequency. The value of  $\theta/\pi$  shows whether the reflected wave will lead or lag the incident wave by  $\theta/\pi$  ranging from 0 to 1. In the initial condition between 40- 320Hz and 700Hz,  $\theta/\pi$  values are close to one, which shows the reflected waves are out of phase from the incident wave. Other values show different value for  $\theta/\pi$ , which indicate the reflected waves differ in phase from the incident wave. In the theoretical study [6], the initial value of phase shows the reflected waves are out of phase from incident waves. With an increase in the frequency, the  $\theta/\pi$  decreases between reflected and incident wave.

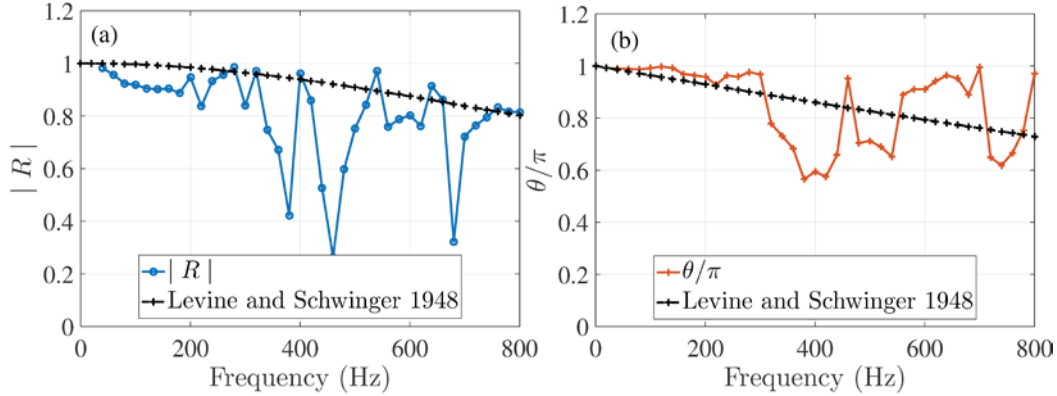


Figure 3 : (a) Variation of modulus of reflection coefficient ( $|R|$ ) with frequency for open end with flanged case at the exit of duct (b) Variation of phase with frequency at open end exit of duct;  $d$  represents the distance between microphones in meter. For frequency range 40-300Hz,  $d=0.4\text{m}$ , for 320-800Hz,  $d=0.2\text{m}$ .

### 3.2 Variation of Reflection coefficient for different area ratio ( $AR$ ) with different air flow rate

For a completely open end duct, the cross-section geometry is a square size of 90X90mm. A variable aperture is fixed at the exit, creates a jump in cross section of duct. The circular opening of the variable aperture is 89mm in diameter. Completely open end with variable aperture corresponds to the  $AR=0.97$ .

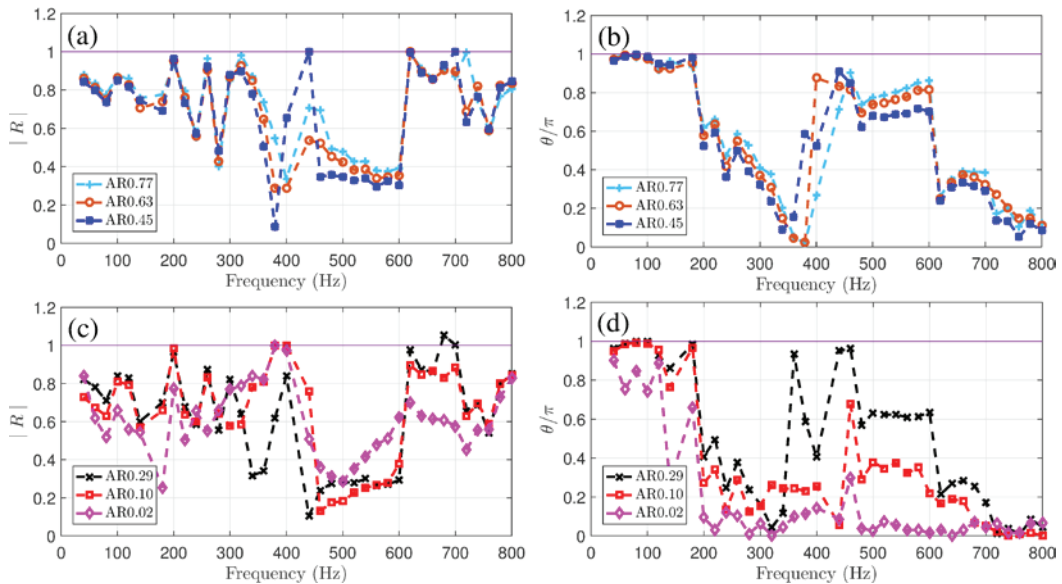


Figure 4(a), (b), (c) and (d) shows the variation of modulus of reflection coefficient and phase difference with air flow rate of 200slpm inside the duct. For frequency range 40-300Hz,  $d=0.4\text{m}$ , for 320-800Hz,  $d=0.2\text{m}$ .

Figure 4 shows the experiment results with the air flow rate of **200slpm** at different  $AR$ . Figure 4 (a)  $|R|$  and (b) shows  $R$  at the exit and the corresponding  $|R|$  phase ( $\theta/\pi$ ) respectively. The value at 160 and 420Hz is ignored because of resonance inside the duct. The reflection coefficient values are very high, which cannot be possible for the present case as no acoustic source is present at the exit of the duct.  $|R|$  for  $AR = 0.77, 0.63$  and  $0.45$  is plotted, which shows with the reduction in  $AR$ , the  $|R|$ -value also decreases.  $|R|$  for  $0.45$  is lesser or equal compared to other  $AR$  until 400Hz. In the

frequency range of 400-460Hz and at 700Hz the  $|R|$ -value is higher compared to other which can be due to resonance in the duct at 200slpm.

In figure 4(b), the phase difference  $\theta/\pi$  between the incident and reflected wave for the frequency range of 40-180Hz, 440-580Hz is higher. On the contrary, other frequency range shows the reflected waves are out of phase. With an increase in frequency above 180Hz, the  $\theta/\pi$  between reflected wave and incident wave decreases. For the frequency range of 340-380Hz, the reflected wave is in phase with incident waves.

Air flow rate plays a significant role in the propagation of acoustic wave inside the duct. In figure 4(c) and (d) shows the plot for  $AR=0.29, 0.10$  and  $0.02$ ,  $|R|$ -value is consistently lower between the ranges of 40-250Hz for lower  $AR$ , with the increase in frequency,  $|R|$ -value increases between 250-620Hz. For 640-800Hz, the  $|R|$ -value is smaller compared to others for lower  $AR=0.02$ . Completely close end creates the condition for the close–close end, and the standing waves are formed for lower  $AR$ .

Figure 4(d) shows the  $\theta/\pi$  plot for the corresponding  $|R|$  with different  $AR=0.29, 0.10$  and  $0.02$ , respectively. For higher  $AR$  the  $\theta/\pi$  values between the frequency range of 40-180Hz, the  $\theta/\pi$  value between reflected and incident wave is close to one as the frequency increases above 200Hz the  $\theta/\pi$  value decreases and reaches the 0 beyond 700Hz. For  $AR=0.02$ , the  $\theta/\pi$  value is higher for the frequency range of 40-180Hz, With an increase in frequency above 200Hz, the  $\theta/\pi$  decrease close to 0 which shows the reflected wave is in the same phase with the incident wave.

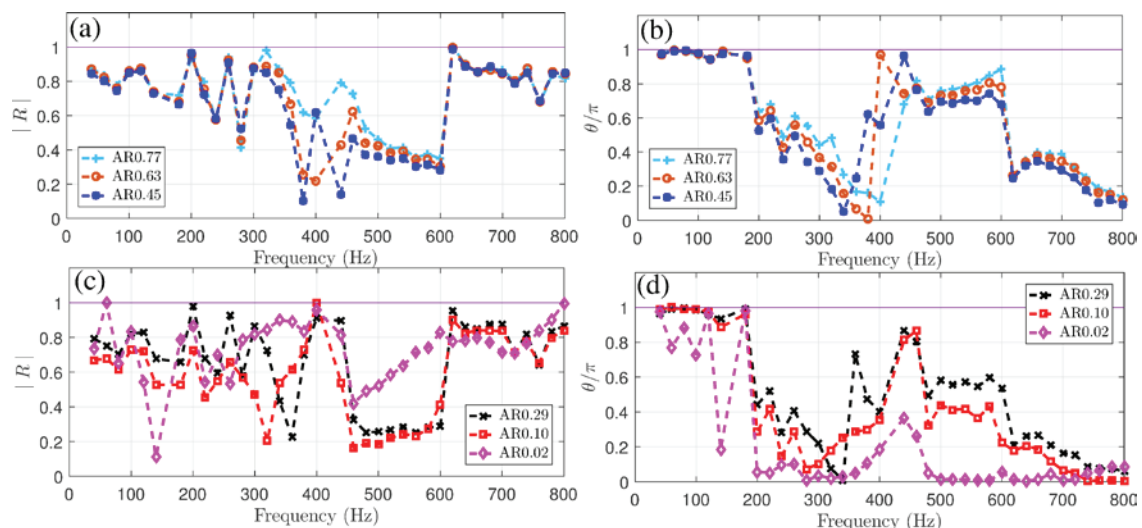


Figure 5(a), (b), (c) and (d) shows the variation of modulus of reflection coefficient and phase difference with air flow rate of 600slpm inside the duct. For frequency range 40-300Hz,  $d=0.4\text{m}$ , for 320-800Hz,  $d=0.2\text{m}$ .

Figure 5(a), (b), (c) and (d) presents the variation of  $|R|$  for **600slpm** air flow rate. In figure 5(a) and (b), for  $AR=0.77, 0.63$  and  $0.45$ , between the frequency range of 300-600Hz,  $|R|$  decreases with a decrease in  $AR$ . At 400Hz, the  $|R|$ -value is almost same for  $AR=0.77$  and  $0.45$ . The variation is similar to 200slpm.

Figure 5(b), shows the same variation as shown in 200slpm for phase. The  $\theta/\pi$  values are close to one, for the frequency range of 40-180Hz and 400-600Hz, as the frequency is increased above 200Hz and 600Hz, the  $\theta/\pi$  value decreases.

Figure 5(c) and (d), the  $AR=0.02$  acts differently compared to 200slpm; it must be noted that at high flow rate with a decrease in  $AR$  a whistling sound is generated at the exit. It may be due to the vortices forming at the exit area because of the low-pressure region behind the aperture. The vortices forming at the exit of the duct creates acoustic waves in upstream as well downstream direction which can alter  $|R|$ -value at the same location. For the higher flow rate at  $AR=0.02$ ,  $|R|$ -value shifts upward. For 600slpm, 40-100Hz, 180-240Hz, 280-340Hz, 400-600Hz, and 740-800Hz,  $AR=0.10$  corresponds to the lowest  $|R|$ -value.

In figure 5(d), the  $\theta/\pi$  values are same as that of 200slpm. The lower  $AR$  shows the reflected waves are in phase with incident waves in the range of 200-350Hz and 480-800Hz. For the case of the other two  $AR$ , the  $\theta/\pi$  value close to one between 40-180Hz, as the frequency is increased, the

$\theta/\pi$  value decreases.

### 3.3 Variation of Reflection coefficient with air flow rate:

In figure 6(a), (b), (c), the Airflow rate does not affect  $|R|$ . The plot shows the same trend for  $|R|$ -value. The decrease in  $AR$  at a higher flow rate will generate vortices outside the duct which make acoustic waves and these acoustic waves' travels in both directions upstream as well downstream. The upstream traveling waves contribute to instability inside the combustor. The whistle sound was observed at the exit for lower  $AR$ , i.e., 0.29, 0.10 and 0.02 during the experiment, which changes the boundary condition at the exit and can contribute to instability as well increase the damage inside the combustor. Figure 6(d) and (f) shows a higher value of  $|R|$  for a higher flow rate. Figure 6(e) shows  $|R|$ -value is higher for lower flow rate 200slpm, which is same as other  $AR$  conditions.

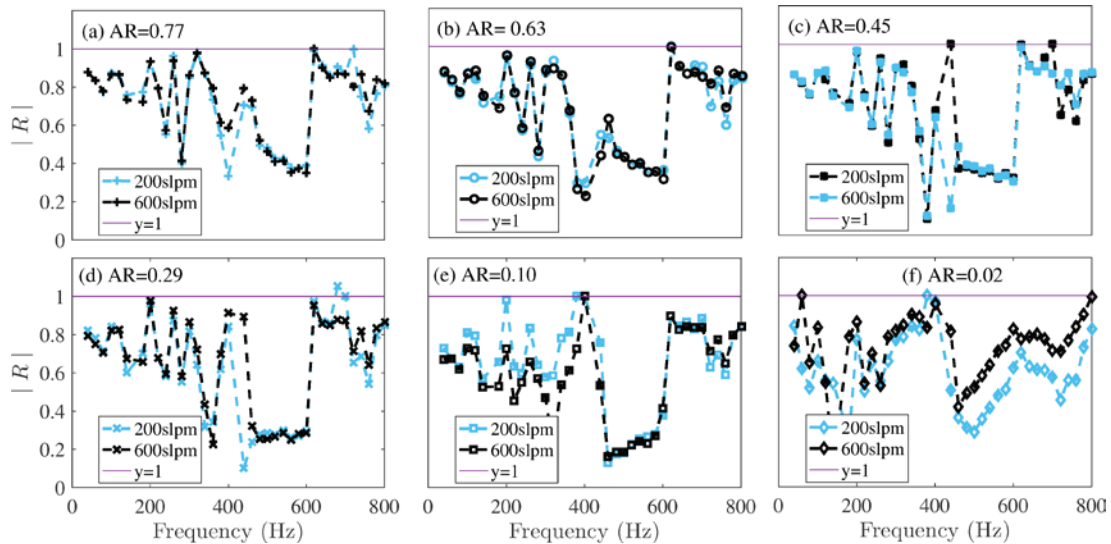


Figure 6(a), (b), (c), (d), (e) and (f) shows the variation of modulus of reflection coefficient for different area ratio with air flow rate of 200 and 600slpm inside the duct. For frequency range 40-300Hz,  $d=0.4m$ , for 320-800Hz,  $d=0.2m$ .

### 3.4 Variation of Reflection coefficient with area ratio (AR) to exit

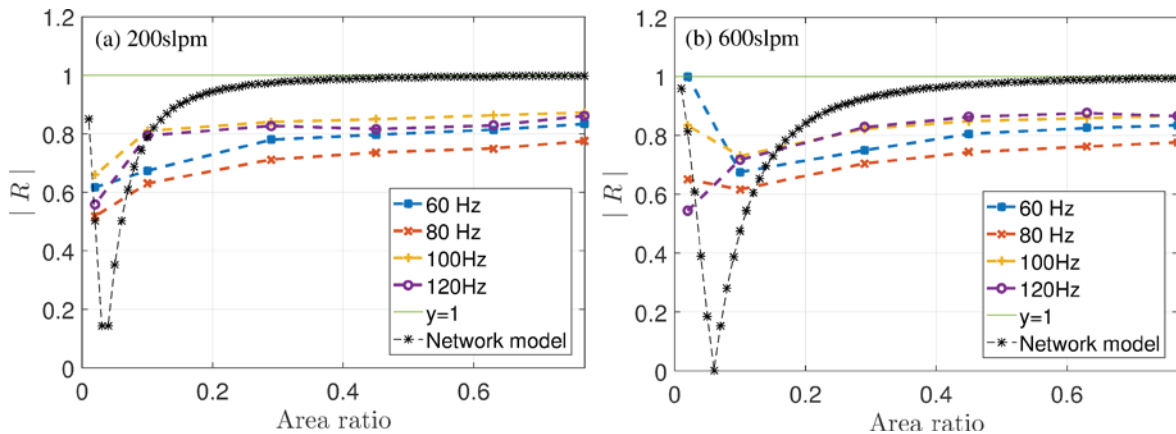


Figure 7(a) and (b) shows the variation of modulus of reflection coefficient with different area ratio for different air flow rate.

Figure 7(a) and (b) shows the variation of  $|R|$  with  $AR$ ,  $AR$  at the exit of the combustor is decreased from 1-0.02. From the plot,  $|R|$  is equal to 1 with the change of  $AR$  from 1 to 0.10. With the decrease in  $AR$  beyond 0.10, the  $|R|$ -value decreases drastically for both the air flow rate. From the numerical model explained in [17] with variation in mean flow, the anechoic condition changes, and its shift to the higher value of  $AR$ . With the increase in air flow rate, the anechoic boundary condition shifts higher as explained earlier and also observed in the experiment with different air flow rate. In gas turbine engine the anechoic boundary condition will change as the flow rate changes will also lead

to change in the mechanism of instability inside the combustor chamber with the crossing of blades at the exit.

#### 4. CONCLUSIONS

The major issue with real-time running of a gas turbine engine is change in boundary with inside and the exit condition. The present study focuses on determining the exit boundary condition.

1. For  $AR > 0.4$ , the  $|R|$  value remains constant for a particular frequency at constant air flow rate. With  $AR$  below 0.10,  $|R|$  decreases drastically, the exit boundary act as the anechoic exit. With the increase in air flow rate, the anechoic boundary at exit shift to the higher value of  $AR$ , which is already discussed in [17] with a network model. The experimental data for an air flow rate of 200slpm and 600slpm shows a similar trend of  $|R|$  as expected from the network model. The anechoic boundary condition can be determined experimentally with a better resolution for  $AR$  at the exit.
2. For higher  $AR=0.77, 0.63, 0.45$  and  $0.29$ , change in air flow rate has no significant effect on  $|R|$ , with the decrease in  $AR$  close to 0.10 and 0.02, the air flow rate plays a vital role in identifying the exit boundary condition, the higher air flow rate has higher value of  $|R|$ . This behavior can also be due to the vortices forming at the exit of combustor because of the low-pressure region.
3. At a particular air flow rate, with the increase in frequency, the  $|R|$  value shows the very random trend, it's neither decreasing nor increasing. On the other hand, it is always less than one, which can be due to the complex geometry of the variable aperture fixed at the exit of the duct.
4. The  $\theta/\pi$  shows the difference between reflected and incident wave inside the duct. In the present investigation, the higher  $AR$  shows that  $\theta/\pi$  variations between 0-1, for lower frequency range the  $\theta/\pi$  values are higher which shows the reflected waves are out of phase from the incident wave. For  $AR=0.02$ , the reflected waves are in phase with incident waves for most of the frequencies.

#### REFERENCES

- [1] Culick FEC, Papparizos L, Sterling J, Burnley V. Combustion noise and combustion instabilities in propulsion systems. AGARD Conf Proc 512 1992.
- [2] Albayrak A, Steinbacher T, Komarek T, Polifke W. Convective Scaling of Intrinsic Thermo-Acoustic Eigenfrequencies of a Premixed Swirl Combustor. Proc ASME Turbo Expo 2017;140:1–11. doi:10.1115/GT2017-64929.
- [3] Hoeijmakers M, Kornilov V, Lopez Arteaga I, de Goey P, Nijmeijer H. Intrinsic instability of flame-acoustic coupling. Combust Flame 2014;161:2860–7. doi:10.1016/j.combustflame.2014.05.009.
- [4] Hoeijmakers M, Kornilov V, Arteaga IL, de Goey P, Nijmeijer H. Flame dominated thermoacoustic instabilities in a system with high acoustic losses. Combust Flame 2016;169:209–15. doi:10.1016/j.combustflame.2016.03.009.
- [5] Murugesan M, Singaravelu B, Kushwaha AK, Mariappan S. Onset of flame-intrinsic thermoacoustic instabilities in partially premixed turbulent combustors. Int J Spray Combust Dyn 2018;10:171–84. doi:10.1177/1756827718758511.
- [6] Levine H, Schvhnger J. Levine - On the Radiation of Sound from an Unfianged Circular Pipe.pdf 1948;73.
- [7] Corporation PP, York N. Investigation of the Reflection of Perturbations from the subsonic part of a Laval nozzle 1975:75–83.

- [8] Johnston JP, Schmidt WE. Measurement of acoustic reflection from an obstruction in a pipe with flow. *J Acoust Soc Am* 1978;63:1455–60. doi:10.2514/6.1976-538.
- [9] Cargill AM. Low-frequency sound radiation and generation due to the interaction of unsteady flow with a jet pipe. *J Fluid Mech* 1982;121:59–105. doi:10.1017/S0022112082001803.
- [10] Poinot T, Le Chatelier C, Candel SM, Esposito E. Experimental determination of the reflection coefficient of a premixed flame in a duct. *J Sound Vib* 1986;107:265–78. doi:10.1016/0022-460X(86)90237-3.
- [11] Davies POAL. Practical flow duct acoustics. *Top Catal* 1988;124:91–115. doi:10.1016/S0022-460X(88)81407-X.
- [12] Norris AN, Sheng C. Acoustic Radiation from a circular pipe with an infinite flange. *J Sound Vib* 1989;135:85–93.
- [13] Duran I, Moreau S. Solution of the quasi-one-dimensional linearized Euler equations using flow invariants and the Magnus expansion. *J Fluid Mech* 2013;723:190–231. doi:10.1017/jfm.2013.118.
- [14] Seybert AF, Ross DF. Experimental determination of acoustic properties using a two-microphone random-excitation technique. *J Acoust Soc Am* 1977;61:1362–70. doi:10.1121/1.381403.
- [15] Bodén H, Åbom M. Influence of errors on the two-microphone method for measuring acoustic properties in ducts. *J Acoust Soc Am* 1986;79:541–9. doi:10.1121/1.393542.
- [16] M. C. A. MP, Hirschberg A, Reijnen AJ, Wijnands APJ. Damping and reflection for an open pipe at low mach and low Helmholtz numbers. *J Fluid Mech* 1993;256.
- [17] Vishwakarma M, Mariappan S. Parametric study of intrinsic thermoacoustic feedback driven instability in a partially premixed combustor 2018:1–4.